The X-Ray/Radio/Flaring Properties of Cygnus X-3

M. L. MCCOLLOUGH[1], K. I. I. KOLJONEN[2], D. C. HANNIKAINEN[2,3]
[1] *CXC/SAO/CfA, Cambridge, MA, U.S.A.*
[2] *Aalto University Metsähovi Radio Observatory, Kylmälä, Finland*
[3] *Tuorla Observatory, Piikkiö, Finland*

ABSTRACT.
Cygnus X-3 is a unique microquasar. Its X-ray emission shows a very strong 4.8-hour orbital modulation. But its mass-donating companion is a Wolf-Rayet star. Also unlike most other X-ray binaries Cygnus X-3 is relatively bright in the radio virtually all of the time (the exceptions being the quenched states). Cygnus X-3 also undergoes giant radio outbursts (up to 20 Jy). In this presentation we discuss and review the flaring behavior of Cygnus X-3 and its various radio/X-ray states. We present a revised set of radio/X-ray states based on Cygnus X-3's hardness-intensity diagram (HID). We also examine the connection of a certain type of activity to the reported AGILE/Fermi gamma-ray detections of Cygnus X-3.

1. Introduction

Cygnus X-3 represents one of the most unusual X-ray binaries to have been observed (see Bonnet-Bidaud & Chardin 1988 for a review). It is at a distance of ~ 9 kpc (Predehl et al. 2000) in the galactic plane and is heavily obscured at optical wavelengths. Cygnus X-3 does not fit well into any of the established classes of X-ray binaries. It has a 4.8-hour orbital period, observed both in the X-ray (Parsignault et al. 1972) and the infrared (Mason et al. 1986), which is typical of a low mass X-ray binary. But infrared spectroscopic observations (van Kerkwijk et al. 1992, Fender et al. 1999) indicate that the mass-donating star is a Wolf-Rayet star making the system a high mass X-ray binary. In addition, Cygnus X-3 undergoes giant radio outbursts and there is strong evidence of jet-like structures moving away from Cygnus X-3 at 0.3–0.9c (Molnar et al. 1988, Schalinski et al. 1995, Mioduszewski et al. 2001; see Fig. 1). The nature of the compact object is uncertain, but recent spectral studies (Szostek et al. 2008; hereafter SZM08 and Hjalmarsdotter et al. 2009) indicate that it may be a black hole.

2. Discoveries from Multi-Wavelength Studies

In studies (McCollough et al. 1997; 1999a, hereafter M99; 1999b) designed to classify Cygnus X-3's spectral states and behavior, the 20–100 keV hard X-ray (HXR) emission detected with *CGRO*/BATSE, was compared with the radio data from the Green Bank Interferometer (GBI; 2.25 and 8.3 GHz) and the Ryle Telescope (15 GHz), and with the 1–12 keV soft X-rays (SXR) detected with the *RXTE*/ASM. Among the discoveries from these comparisons were:

(a) During times of moderate radio brightness (~ 100 mJy) and low variability, the HXR flux anti-correlates with the radio. It is during this time that the HXR reaches its highest level (see Fig. 2).

(b) During periods of flaring activity in the radio the HXR flux switches from an anti-correlation to a correlation with the radio. In particular, for major radio flares and the quenched radio emission (very low radio fluxes of 10–20 mJy) which precedes them the correlation is strong (see Fig. 2).

(c) The HXR flux has been shown to anti-correlate with the SXR. This occurs in both the low and high SXR states (see Fig. 3).

(d) Results showing that flaring periods in the radio occur during the high SXR states (Watanabe's 1994) were also confirmed.

(e) It has been found from the *CGRO*/BATSE and *CGRO*/OSSE data that the spectrum of Cygnus X-3 (in the 20–100 keV band) becomes harder during times of radio flaring (McCollough 1999b).

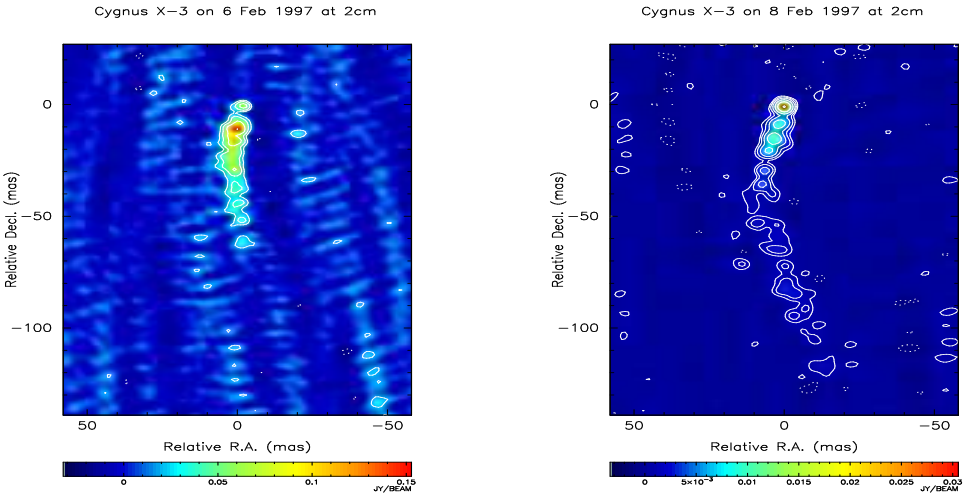

Fig. 1. VLBI radio images obtained during a major radio flare of Cygnus X-3 (Mioduszewski et al. 2001). The *left* panel shows a one-sided radio jet a few days after the peak in the radio. The *right* panel shows how the jet has evolved two days later.

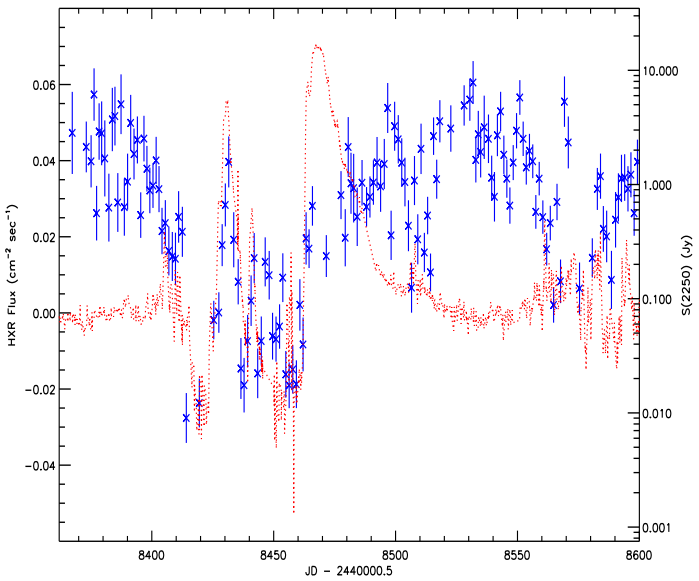

Fig. 2. A comparison of GBI 2.25 GHz radio emission (red) with the *CGRO*/BATSE HXR emission (blue) from M99. Note the anti-correlation during times of radio quiescence and the switch to a correlation during periods of quenched emission and major radio flares.

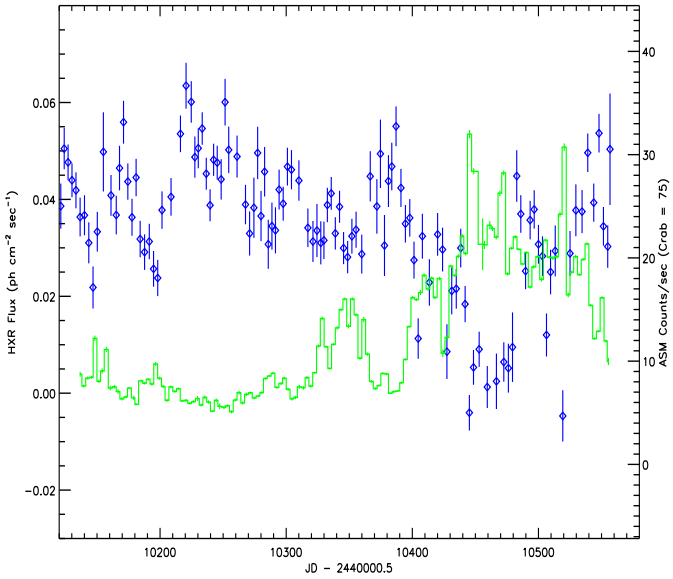

Fig. 3. A comparison of *RXTE*/ASM SXR emission (green solid line) with the *CGRO*/BATSE HXR emission (blue diamonds) from McCollough et al. 1997. Note the anti-correlation during all types of activity.

3. Cygnus X-3 Radio/X-Ray States

The X-ray spectra of Cygnus X-3 are notoriously complex (see Section 5 and Fig. 6). Cygnus X-3 exhibits the canonical X-ray states seen in other X-ray binaries (XRBs), namely the high/soft (HS) and low/hard (LH) states, in addition to the intermediate, very high and ultrasoft states (e.g. Szostek & Zdziarski 2004, hereafter SZ04; Hjalmarsdotter et al. 2009). However, in Cygnus X-3, the strong radio emission is also classified into states of its own (Waltman et al. 1996; M99). The X-ray emission has been found to be linked to radio emission in Cygnus X-3. M99 found that during periods of flaring activity in the radio the hard X-ray flux switches from an anti-correlation to a correlation with the radio. In addition, the HXR flux has been shown to anti-correlate with the soft X-rays in both canonical X-ray states (McCollough et al. 1997). Recently these X-ray and radio states were implemented into a more unified picture presented in SZM08: the radio/X-ray states (see Fig. 4 and Table 1).

4. Cygnus X-3's Hardness-Intensity Diagram

Following from previous work on black hole transients (Fender et al. 2004) a hardness-intensity diagram (HID) may yield insight into the nature of Cygnus X-3 despite it not being a transient in the strict sense of the word. Thus, using *RXTE* pointed observations, we constructed a HID (Koljonen et al. 2010) to study the behavior of Cygnus X-3. The bands we used were chosen to probe different emission regions, with the SXR ($3-6$ keV) range representing the accretion disk and the HXR ($10-15$ keV) range representing the Comptonized part of the spectrum. Given that Cygnus X-3 is also a persistent radio source we can add an additional dimension to the HID. For each of the data points plotted we have used radio data from either GBI or the Ryle radio telescope to color code each data point by its radio flux density. The resulting plot is shown in Fig. 5.

At first glance the plot appears surprisingly similar to other black hole XRB HIDs,

TABLE I
Different Classification Methods of Cygnus X-3's States and Spectra (Koljonen et al. 2010)

Canonical X-ray States	Radio States	SZ04 States group:	SZ04 States name:	SZM08 States	New States
low/hard	quiescent	1	hard	quiescent	quiescent
		2	intermediate	minor flaring	transition
intermediate	minor flaring	3	very high	suppressed "post-flare"	FHXR
high/soft	major flaring quenched	4	soft non-thermal	major flaring	FIM
		5	ultrasoft	quenched	FSXR hypersoft

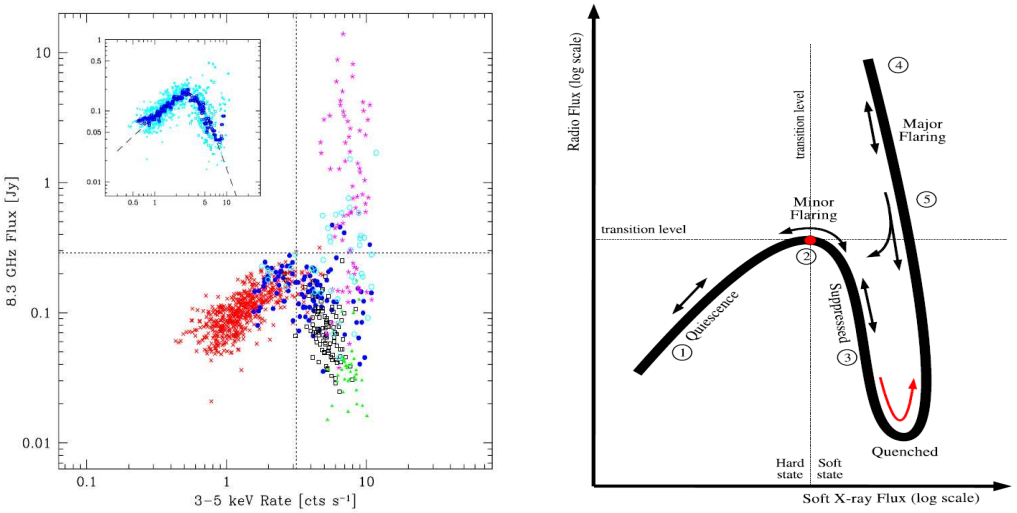

Fig. 4. *LEFT:* X-ray (*RXTE*/ASM: 3–5 keV) vs. radio (GBI: 8.3 GHz) plot with with different regions/states color coded (see SZM08 for full details). *RIGHT:* A cartoon of the X-ray - radio plot with states and paths between states labeled (SZM08).

but there are some very important differences. First of all, Cygnus X-3 does not show hysteresis in the HID (Hjalmarsdotter et al. 2009) but simply increases in intensity as the spectrum softens. In black hole XRBs the LH state is present throughout the right branch, whereas in Cygnus X-3 the LH state is confined to the foot of the Q. The right branch in this case is dominated by X-ray flaring in Cygnus X-3. In addition, the flaring data are also spread into different hardnesses which wholly fill the inside area of the Q.

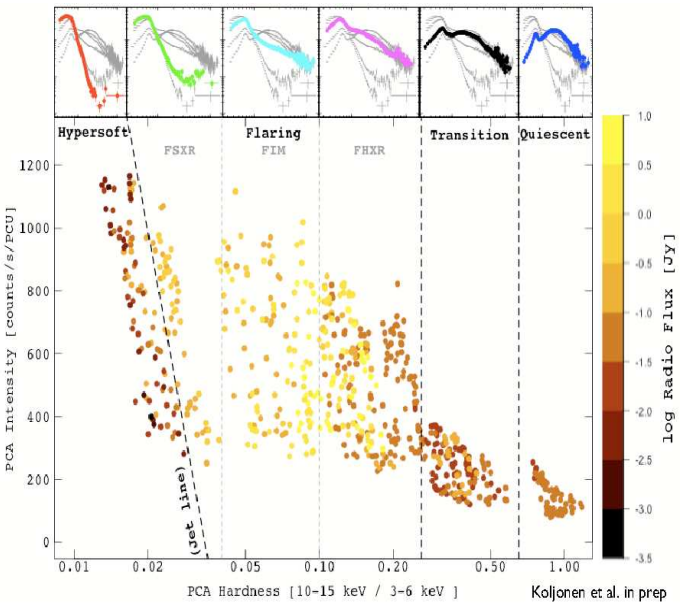

Fig. 5. A HID for Cygnus X-3 created from pointed RXTE observations which also have associated radio observations (Koljonen et al. 2010). The color of the data points represents the radio flux on a logarithmic scale. Across the top of the plot are average spectra for the labeled regions.

5. Cygnus X-3's Spectra

Cyg X-3 has a complex spectrum that can show drastic changes with change in spectral state. Among the spectral components are: (a) disk blackbody emission; (b) thermal Comptonized emission; (c) non-thermal Comptonized emission; (d) line emission; and (e) internal and external absorption. Fig. 6 shows the succession of Cygnus X-3 spectra as it progresses from a quiescent state (1), which is dominated by thermal Comptonized emission, to a quenched state (6) in which the disk blackbody emission is prominent. The intermediate spectra have a strong non-thermal Comptonized emission component that appears as a power law tail to the spectrum and is most likely tied into the major radio flares.

6. New State Classification

An examination of Cygnus X-3's HID allows us to create a revised set of radio/X-ray states based on X-ray hardness and/or radio flux. We have divided them into three distinct areas which we call quiescent, flaring and hypersoft.

`Quiescent:` The quiescent represents a region of moderate radio brightness, low variability, and an X-ray spectrum which is dominated by thermal Comptonized emission which peaks at around 20 keV and a prominent Fe line complex around 6.7 keV. We have divided this region into two sub-regions: *quiescent* and *transition*. These sub-regions represent a gradual decrease and flattening of the hard part of the spectrum.

`Flaring:` In turn the flaring state can be broken down into three sub-states according to X-ray hardness and the shape of the spectra: flaring/soft X-ray (*FSXR*), flaring/intermediate (*FIM*), and flaring/hard X-ray (*FHXR*). The right-hand side of the *FHXR* is where the minor flaring activity occurs. From the center of the *FHXR* through the *FIM* is the area where one finds the major radio flaring activity. Finally the *FSXR*

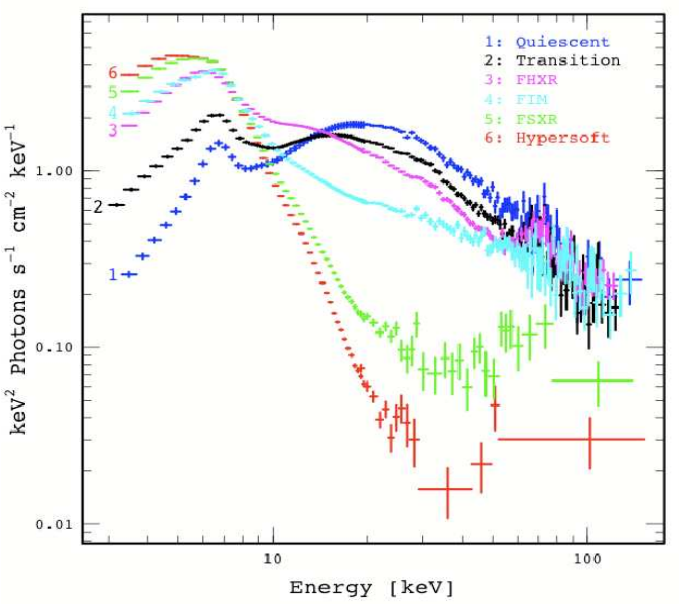

Fig. 6. Plotted are typical *RXTE* X-ray spectra for Cygnus X-3 (Koljonen et al. 2010). They range from a quiescent state (1-2) with a strong thermal Comptonized spectrum through the various flaring states (3-5) with their non-thermal Comptonized spectral tail to finally the hypersoft (6) spectrum whose emission is dominated by thermal disk emission. Note the spectral pivoting around 10 keV.

represents an area where major radio flares occur but the HXR flux has been greatly reduced. This may indicate a type of flare where there has been a strong interaction with Cygnus X-3's wind.

`Hypersoft:` Finally there is the *hypersoft* state where a large fraction of the emission is from a disk blackbody and the non-thermal tail is an order of magnitude weaker (if present) than in the *FSXR*. The radio emission is highly suppressed (unless a previous major radio flare is still decaying). This is also what is known as the *quenched* state. This state is a precursor to the production of a major radio flare.

In Figs. 5 and 6 display the location in the HID and typical spectra for these states. In Table 1 the states and spectra of Cygnus X-3 from various studies have been listed. It should be noted that as one goes down the table there is a general transition in the behavior of Cygnus X-3. But Cygnus X-3 can loop between states and also rapidly proceed between an upper state to a lower state while only spending minimal time in the intermediate states.

7. The *Hypersoft* State and γ-Ray Emission

During the quenched state, the radio emission falls to very low values ($1-20$ mJy), the HXR vanishes, and SXR reaches very high values. As noted above this is a precursor for the occurrence of major radio flares. We have re-examined the X-ray spectra taken during quenching activity and shown that they can be divided into what we call *FSXR* (or ultrasoft of SZ04) and *hypersoft* state. This *hypersoft* state has a power law tail which is an order of magnitude fainter than that found in the quenched state of SZM08 (see Fig. 6 and 7).

Recent observations of γ-ray emission (Tavani et al. 2009, Abdo et al. 2009) from

Cygnus X-3 have shown that the γ-ray emission appears to be directly related to the activity associated with the *hypersoft* state and in turn the occurrence of major radio flares in Cygnus X-3.

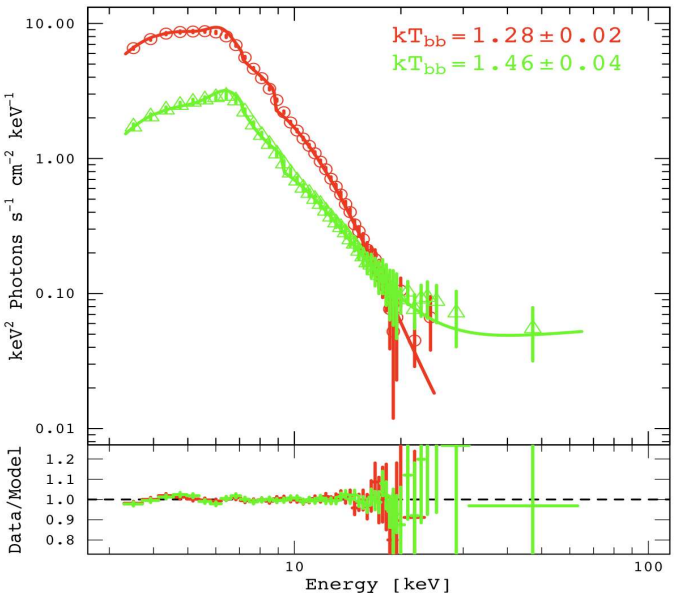

Fig. 7. Plot are of a *FSXR* state (green open triangles) and a *hypersoft* state (red open circles) spectra along with their spectra fits. Note that for the *hypersoft* state the hard X-ray tail and disk blackbody temperature is noticeably lower.

8. Conclusions

We have discussed the various correlations and radio/X-ray states of Cyg X-3.

From the construction of a unique HID for Cygnus X-3 with the radio flux as a third dimension we have gained additional insight into the nature and behavior of Cygnus X-3. We have identified three broad states and several sub-states which are delineated by intensity, X-ray hardness, and radio flux. We have also identified a "new" very soft state that we call the *hypersoft* state. This state directly relates to the γ-ray emission that has been observed from Cyg X-3 (Tavani et al. 2009, Abdo et al. 2009). This analysis lays the groundwork for a much better understanding of the workings and nature of Cygnus X-3.

9. Acknowledgments

MLM wished to acknowledge support from NASA under grant/contract NNG06GE72G, NNX06AB94G and NAS8-03060. KIIK gratefully acknowledges a grant from Jenny ja Antti Wihurin säätiö and Academy of Finland grant (project num. 125189). DCH acknowledges Academy of Finland grant (project num. 212656).

References

Abdo, A. A., et al., 2009 *Science* **326**, 1512
Bonnet-Bidaud, J. M. & Chardin, G. 1988, *Physics Reports*, **170**, 326

Fender, R. P., Gallo E., & Belloni, T. E. 2004 *Mon. Not. R. Astr. Soc.* **355**, 1105
Hjalmarsdotter L. , et al. 2009, *Mon. Not. R. Astr. Soc.* **,**, 392251
Koljonen, K.I.I. et al. 2010, *Mon. Not. R. Astr. Soc.* **(submitted)**, version.1
Mason, K.O. et al. 1986, *Astrophys. J.* **309**, 700
McCollough, M. L. et al. 1997, *4th Compton Symposium*, AIP Conf. Proc., 410, 813
McCollough, M. L., et al., 1999a, *Astrophys. J.* **517**, 951 (M99)
McCollough, M. L. et al. 1999b, *Astro. Lett. and Comm.*, **38**, 105
Mioduszewski, A. J. et al. 2001, *Astrophys. J.* **553**, 766
Molnar, L. A. et al. 1988, *Astrophys. J.* **331**, 494
Parsignault D. R., et al. 1972, *Nat. Phys. Sci.*, **239**, 123
Predehl P. et al. 2000, *Astron. Astrophys.* **357**, L25
Schalinski, C. J. et al. 1995, *Astrophys. J.* **447**, 752
Szostek, A. & Zdziarski, A. A. 2004, preprint (astro-ph/0401265) (SZ04)
Szostek, A., Zdziarski, A. A. & McCollough, M. L. 2008, *Mon. Not. R. Astr. Soc.* **388**, 1001 (SZM08)
Tavani, M. et al. 2009, *Nature* **462**, 620
van Kerkwijk, M. H. et al. 1992, *Nature* **355**, 703
Waltman, E. B. et al. 1996, *Astron. J.* **112**, 2690
Watanabe, H. et al. 1994, *Astrophys. J.* **433**, 350